Optical Engineering

OpticalEngineering.SPIEDigitalLibrary.org

Comparative study of two ballistic imaging methods based on the femtosecond optical Kerr gate and spatial filtering

Shichao Xu
Wenjiang Tan
Jinhai Si
Pingping Zhan
Junyi Tong
Xun Hou

SPIE.

Comparative study of two ballistic imaging methods based on the femtosecond optical Kerr gate and spatial filtering

Shichao Xu,[a] Wenjiang Tan,[a,*] Jinhai Si,[a] Pingping Zhan,[a] Junyi Tong,[b] and Xun Hou[a]
[a]Xi'an Jiaotong University, Key Laboratory for Physical Electronics and Devices of the Ministry of Education, Shannxi Key Laboratory of Information Photonic Technique, School of Electronic and Information Engineering, No. 28, Xianning West Road, Xi'an 710049, China
[b]Xi'an University of Technology, Department of Applied Physics, No. 5, South Jinhua Road, Xi'an 710048, China

Abstract. We demonstrated two ballistic imaging for an object hidden behind turbid media using the optical Kerr gate (OKG) and spatial filtering (SF), respectively. The influence of the scattering parameters of the turbid media on the image contrast was investigated. The experimental results showed that the image contrast of the SF imaging decreased significantly with increasing optical density and scattering particle size of the turbid media. Compared to the SF imaging, the OKG imaging showed a higher and more stable image contrast as scattering photons in the optical gated imaging case were more effectively eliminated. [DOI: 10.1117/1.OE.53.9.093102]

Keywords: ballistic imaging; optical Kerr gate; spatial filtering; turbid media.

Paper 140569 received Apr. 4, 2014; revised manuscript received Jun. 27, 2014; accepted for publication Aug. 14, 2014; published online Sep. 9, 2014.

1 Introduction

Ballistic imaging based on an ultrafast optical Kerr gate (OKG) was first demonstrated by Alfano et al. for the visualization of objects hidden behind turbid media.[1] Recently, a ballistic imaging technique has attracted great interest in investigating biological tissues,[2] liquid jets,[3] and high-speed fuel sprays.[4] As mentioned in Ref. 1, when a laser pulse transits such a highly turbid media over a straight course, most of the photons participate in multiple scattering interactions. The numerous scattered photons take the longest path in the turbid media and seriously degrade the quality of image as imaging noise. Only a few of photons, called ballistic photons, pass through in a straight line without being scattered. The ballistic photons take the essential information of the object in the turbid media. Additionally, some slightly scattered photons, called snake photons, are minimally disturbed through the scattering media and can also be used in imaging. Thus the critical problem in ballistic imaging is selecting the ballistic and snake photons and eliminating the scattering photons.[1,5,6]

In view of the above, image-bearing photons consist of ballistic photons and snake photons which take shorter path than diffuse photons. Therefore, OKG imaging employed a short time gate with which to observe the object hidden in the turbid media; these methods have been widely investigated.[7–10] On the other hand, the scattered photons could scatter over wide angles relative to the direction of the ballistic photons. The ballistic, snake, and scattering photons belong to different spatial frequency components on the Fourier-transform spectrum plane of the collection lens in the imaging system.[11] Ballistic and snake photons are formed at the central frequency region of the Fourier-transform spectrum plane as low-frequency components. Therefore, spatial-filtering (SF) imaging using a low-pass filter (LPF) could improve the visibility of an object in turbid media.[11–13] Moreover, the combination of OKG imaging and SF imaging has also been demonstrated to more effectively improve the visibility of objects hidden in turbid media.[14] In OKG imaging, a transient aperture could be usually induced because of the nonlinear optical effect between the pump beam and the optical Kerr medium, and the SF resulting from the transient aperture would act on the optical imaging along with the OKG. However, for OKG imaging and SF imaging, the scattering parameters of the turbid media have different influences on the image contrast, therefore, the understanding of these influences is important for their applications.[15]

In this paper, we demonstrated the performance of OKG imaging and the SF imaging for different turbid media, respectively. The experimental results showed that the image contrast of the SF imaging significantly decreased with increasing optical density (OD) and scattering particle size of the turbid media. Compared to the SF imaging, a higher and more stable image contrast can be obtained with the OKG imaging technique. This study indicated that OKG imaging was an effective method for highly turbid media.

2 Experimental Setup

Figure 1(a) shows the experimental setup scheme of ballistic imaging using the OKG. A Ti:Sapphire laser system (Coherent Inc., Santa Clara, California, Libra-USP-HE) emitting 50 fs laser pulses centered at 800 nm at a repetition rate of 1 kHz was used in our experiments. The output of the laser beam was split into two beams by a short-pass filter (SPF: Newport Inc., Santa Clara, California, 10SWF-800-B). The central wavelengths of the two beams were about 780 and 800 nm, respectively. Passing through a variable optical delay line, the short wavelength part was focused onto an

*Address all correspondence to: Wenjiang Tan, E-mail: tanwenjiang@mail.xjtu.edu.cn

0091-3286/2014/$25.00

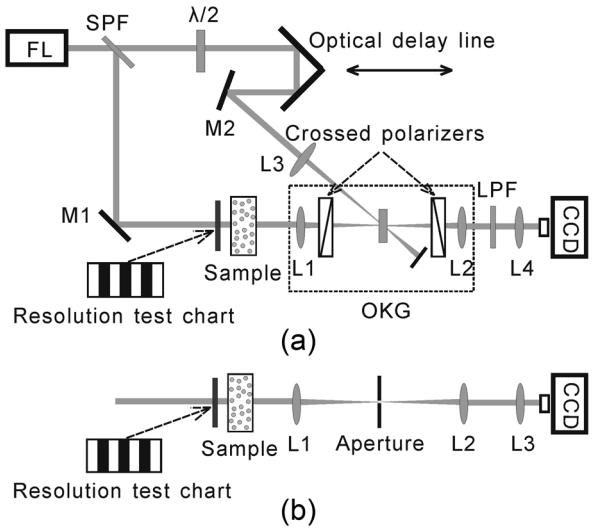

Fig. 1 Experimental setup scheme of ballistic imaging: (a) the optical Kerr gate (OKG) imaging and (b) the spatial-filtering (SF) imaging. FL, femtosecond laser; SPF, short-pass filter; LPF, long-pass filter; $\lambda/2$, half-wave plate; M, mirror; and L, lens.

optical Kerr medium as the gating beam by a lens (L3). A half-wave plate was introduced into the gating beam to make the angle of the polarizations between the pump and the probe beams $\pi/4$ for maximum gating efficiency.

The long wavelength part was reflected by the SPF and passed through a turbid media as the probe beam, which was modulated by a resolution test pattern (a United States Air Force contrast target) before the sample cell. The disturbed photons were collected by a 10-mm focal-length lens (L1) and passed through the OKG which consisted of a pair of polarizers with a Kerr material between them. A 1-mm thickness tellurite glass was used as the Kerr medium and was placed at the back focal plane of L1. Since the nonlinearity of the tellurite glass mainly originated from the electronic polarization, the tellurite glass has a nonlinear response time as short as tens of femtoseconds.[16] In the OKG imaging system, the laser pulse was broadened by the complex elements and the full-width at half-maximum of the time-resolved optical Kerr signals of the tellurite glass was measured to be about 200 fs.[9] Moreover, the tellurite glass has a large nonlinear refractive index of $\sim 10^{-15}$ cm^2/W and a wide transparency window of 400 to 2000 nm. Thus, the tellurite glass could offer high temporal resolution, high signal-to-noise ratio, and a wide applicable wavelength range for the OKG imaging. By adjusting the optical delay line, the multiply scattering photons were suppressed and the ballistic photons were imaged with a high resolution CCD camera (Lumenera Inc., Canada, Ottawa, INFINITY 3-1). A LPF (Newport Inc., 10LWF-800-B) was inserted before the CCD and was used to eliminate noise photons generated by the gating beam scattering in the Kerr medium. In this experiment, the turbid media were monodispersive suspensions of polystyrene microspheres (Sphere Scientific Co., Ltd., China, Wuhan) in deionized water, and were filled into a 1-cm path length sample cell. The ODs of different turbid media were controlled by adjusting the concentrations of polystyrene microspheres suspensions and were measured by the collimated transmittance approach with a detection acceptance angle of 0.16 deg.[17]

The optical system of SF imaging was set up by replacing the Kerr medium with an aperture at the back focal plane of the L1, as shown in Fig. 1(b). Without turbid media, the diameter of the laser beam at the back focal plane of L1 was measured to be about 260 μm (intensity decay $1/e^2$) using the knife-edge method.[18] This meant that the spot size of the ballistic photons on the Fourier-transform spectrum plane was about 260 μm. To avoid a blurred image due to small aperture blocking of the high-frequency component of the image, we used an aperture with a diameter of 300 μm in the SF imaging system. It should be noted that the pump beam was also able to induce a transient aperture with the nonlinear optical effect in the OKG, and the OKG was actually a combined temporal and spatial gate. Therefore, to truly present the different performances of the OKG imaging and the SF imaging, the spot size of the pump beam at the Kerr medium was set to be about 340 μm in the OKG imaging system.

3 Experimental Results and Discussion

Figure 2 shows a typical imaging result under different conditions with the suspensions of 15.0 μm polystyrene microspheres. Without the SF or the OKG, the object was directly imaged and is shown in Fig. 2(a). The image of the object is seriously disturbed due to the number of scattered photons that were imaged as noise. Figure 2(b) shows the image of the object hidden in the turbid media using the SF. The object was rendered visible by eliminating part of the scattered photons, but the contrast of the image was still unsatisfactory. Figure 2(c) shows the time-gated ballistic imaging using the OKG. We found that the OKG imaging greatly improved the visualization of the object because the OKG eliminated the scattered photons very well.

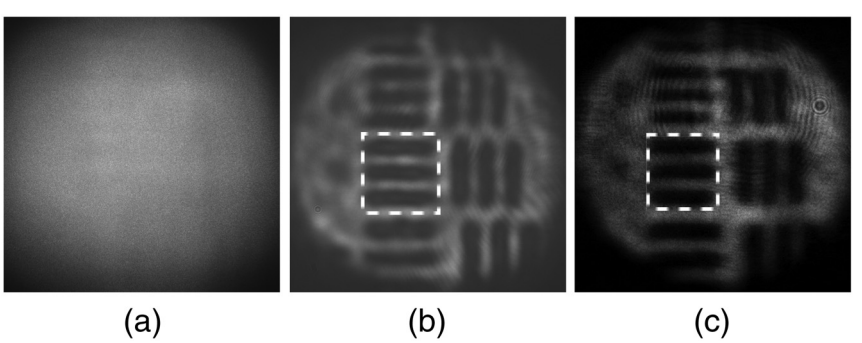

Fig. 2 Comparison of the images of object under the different conditions: (a) direct imaging without the SF or the OKG, (b) SF imaging, and (c) OKG imaging.

To further quantitatively evaluate the performance of the two ballistic imaging techniques, we calculated the contrast of images in a 1.41-line pair/mm section of the resolution test pattern as shown in the boxes of Fig. 2. The contrast of the images was calculated with the following formula contrast $= (I_1 - I_2)/(I_1 + I_2)$, where I_1 is the average image intensity of the unshadowed parts in the square-wave pattern region and I_2 is the average image intensity of the shadowed parts in the square-wave pattern region.

Figure 3 shows the contrast of images for the OKG imaging, the SF imaging and the direct imaging for the turbid media of 0.4, 3.1, and 15.0 μm polystyrene microspheres suspensions, respectively. We can see that the contrast of images for the direct imaging is much smaller than that for the OKG imaging and SF imaging at the same ODs. With increasing scattering particle size, the contrast of the images for the direct imaging gradually became poor. For the 0.4 μm polystyrene microspheres suspensions, the contrast of the images was about 0.30 when varying the ODs from 8.3 to 11.6. The contrast of the images decreased from 0.40 to 0 when varying the ODs from 6.3 to 9.6 for the 3.1 μm polystyrene microspheres suspensions. The contrast of the images was almost zero for the 15.0 μm polystyrene microspheres suspensions. This occurred because, according to the Mie theory, the probability of angular distribution of scattering photons was different for these turbid media.[19,20] Figure 4 shows these polar plots using a logarithmic scale of scattered intensity versus scattering angle for different diameters of the polystyrene microspheres. The refractive index of the scattering particles (polystyrene microspheres) and the surrounding medium (distilled water) was set to be 1.58 and 1.33, respectively. For 0.4 μm polystyrene microspheres, the probability of angular distribution of the scattering photons is relatively homogeneous versus the scattering angle. But with increasing scattering particle size, the probability of angular distribution of the scattering photons exhibits a strong forward-scattering peak. These residual forward-scattered photons could be collected for the turbid media with increasing scattering particle sizes for a direct imaging method at the same OD.

Compared with direct imaging, a higher contrast of the image can be acquired using the SF imaging for the three turbid media. Due to the different spatial distributions at the spatial Fourier-spectrum plane, the ballistic photons transmitted through the aperture and parts of the scattering photons can be eliminated by the SF. Thus the contrast of the image acquired with the SF was improved. However, the contrast of the images for the SF imaging was significantly decreased with increasing OD and scattering particle size. For the turbid media of 0.4 μm polystyrene microspheres suspensions, the contrast of the images decreased from 0.74 to 0.59, and the contrast of the images decreased from 0.80 to 0.36 for the turbid media of 3.1 μm polystyrene microspheres suspensions. Also, the contrast of the images decreased from 0.53 to 0.10 when varying the ODs from 6.2 to 9.3 for the turbid media of 15.0 μm polystyrene microspheres suspensions. The results shows that although the aperture of the SF imaging system could block most of the scattering photons, some paraxial scattering photons

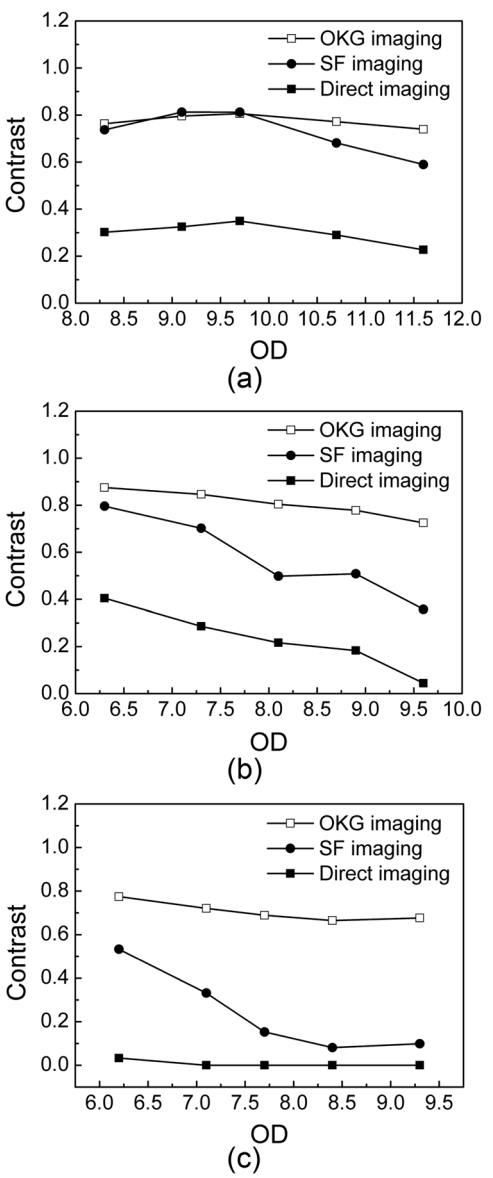

Fig. 3 Contrast of images for different imaging methods and diameter of scattering particles versus ODs: (a) 0.4 μm, (b) 3.1 μm, and (c) 15.0 μm.

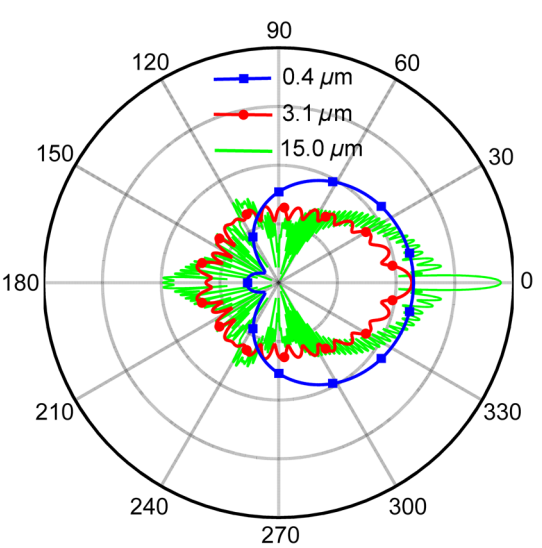

Fig. 4 Polar plots of scattered intensity versus scattering angle for 0.4, 3.1, and 15.0 μm microspheres, respectively.

were still able to transfer through the optical train and were imaged on the CCD. Moreover, the residual paraxial scattering photons increased with increasing OD and the scattering particles size of the turbid media due to increased numbers of the forward-scattering photons.

For the OKG imaging, the contrast of the images decreased from 0.76 to 0.74, from 0.87 to 0.73, and from 0.77 to 0.67 for the turbid media of 0.4, 3.1, and 15.0 μm polystyrene microspheres suspensions, respectively. Because of the temporal and spatial gate effects of the OKG, the scattered photons can be more effectively eliminated in the OKG imaging system. Thus the contrasts of images for the OKG imaging were much higher and more stable than that for the SF imaging. The experimental results showed that the OKG imaging was a promising imaging technique for highly turbid media and the image contrast was superior to that of the SF imaging. It should be also noted that the contrast of the images for the OKG imaging experienced a slight decrease with increasing OD. We attribute this to the influence of the scattering photons from the gating beam when the ballistic photons were scarce in the highly turbid media.

In order to eliminate these scattering gating photons, an SF was inserted before the CCD camera in the OKG imaging system. The SF was composed of two 10-mm focal length lenses and a 1-mm diameter aperture at the confocal plane. Figure 5(a) shows the contrast of the images using the compound imaging system. The turbid media used here were the monodisperse suspensions of 15.0 μm polystyrene microspheres. We can see that the contrast of the images for the compound imaging were all above 0.80 when varying the ODs from 6.3 to 9.2, but the contrast of the image decreased from 0.77 to 0.67 for the OKG imaging in Fig. 3(c). Moreover, the intensity of the images for the compound imaging is also shown in Fig. 5(b), and is well fitted by an exponential function. The experimental result conforms very well to the Beer–Lambert relation, demonstrating that all of scattered photons were efficiently rejected by the combined imaging system.

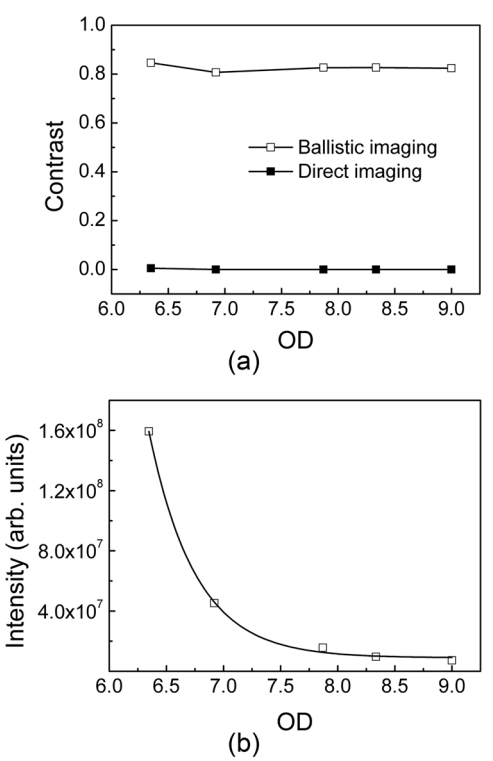

Fig. 5 The contrast and intensity of the images using the combination of the OKG and SF at different ODs: (a) contrast of the images and (b) intensity of the images.

It should be noted that the suspensions of polystyrene microspheres used in our experiment could be used to simulate practical scattering environments, such as biological tissues and fuel sprays of engines. For these strong scattering environments, the OKG imaging method has important potential applications because it more effectively eliminated the scattered photons. The SF imaging system is more suitable for applications in weak scattering environments.

4 Conclusions

In conclusion, we demonstrated a ballistic imaging technique for an object hidden behind turbid media based on the femtosecond OKG and SF. Based on the two methods, we studied the influences of both the ODs and scattering particle sizes of the turbid media on the image contrast. The experimental results indicated that, compared with the direct imaging, the image contrast of the SF imaging was improved for a given OD because part of the scattering photons can be eliminated by the SF at the spatial Fourier-spectrum plane. But the image contrast of the SF imaging significantly decreases with increasing OD and scattering particles size of the turbid media because of the increased residual paraxial scattering photons. Also, a higher and more stable image contrast can be obtained for the OKG imaging because the temporal and spatial gate effects of the OKG more effectively eliminates more scattered photons. For eliminating the residual scattering gating photons, an SF was inserted before the CCD camera in the OKG imaging system, which further improved the contrast of the image.

Acknowledgments

The authors gratefully acknowledge the financial support for this work provided by the National Natural Science Foundation of China under the Grant Nos. 61235003, 61308036, and 61205129, the National Basic Research Program of China (973 Program) under the Grant No. 2012CB921804, the Natural Science Basic Research Plan in Shaanxi Province of China (Program No. 2012JQ8002), and the China Postdoctoral Science Foundation funded project (No. 2013M540753).

References

1. L. Wang et al., "Ballistic 2-D imaging through scattering walls using an ultrafast optical Kerr gate," *Science* **253**(5021), 769–771 (1991).
2. J. Selb et al., "Time-gated optical system for depth-resolved functional brain imaging," *J. Biomed. Opt.* **11**(4), 044008 (2006).
3. S. Idlahcen et al., "Sub-picosecond ballistic imaging of a liquid jet," *Exp. Fluids* **52**(2), 289–298 (2012).
4. D. L. Sedarsky et al., "Fast-framing ballistic imaging of velocity in an aerated spray," *Opt. Lett.* **34**(18), 2748–2750 (2009).
5. F.-X. d'Abzac et al., "Experimental and numerical analysis of ballistic and scattered light using femtosecond optical Kerr gating a way for the characterization of strongly scattering media," *Opt. Express* **20**(9), 9604–9615 (2012).
6. D. Contini et al., "Imaging of highly turbid media by the absorption method," *Appl. Opt.* **35**(13), 2315–2324 (1996).
7. J. B. Schmidt et al., "Ultrafast time-gated ballistic-photon imaging and shadowgraphy in optically dense rocket sprays," *Appl. Opt.* **48**(4), B137–B144 (2009).
8. E. Manuel et al., "Time-gated backscattered ballistic light imaging of objects in turbid water," *Appl. Phys. Lett.* **86**(1), 011115 (2005).

9. W. Tan et al., "Femtosecond nonlinear optical property of a TeO_2-ZnO-Na_2O glass and its application in time-resolved three-dimensional imaging," *Opt. Commun.* **291**, 337–340 (2013).
10. M. E. Paciaroni and M. A. Linne, "Single-shot, two-dimensional ballistic imaging through scattering media," *Appl. Opt.* **43**(26), 5100–5109 (2004).
11. M. Shih and E. Leith, "Spatial filtering of first-arriving light," *Appl. Opt.* **34**(8), 1310–1313 (1995).
12. L. Wang, P. P. Ho, and R. R. Alfano, "Time-resolved Fourier spectrum and imaging in highly scattering media," *Appl. Opt.* **32**(26), 5043–5048 (1993).
13. Q. Z. Wang et al., "Fourier spatial filter acts as a temporal gate for light propagating through a turbid medium," *Opt. Lett.* **20**(13), 1498–1500 (1995).
14. J. Tong et al., "High time-resolved imaging of targets in turbid media using ultrafast optical Kerr gate," *Chin. Phys. Lett.* **29**(2), 024207 (2012).
15. P. Zhan et al., "The influences of turbid media properties on object visibility in optical Kerr gated imaging," *Laser Phys.* **24**(1), 015401 (2014).
16. R. W. Boyd, *Nonlinear Optics*, 3rd ed., Academic Press, Singapore (2008).
17. J. Tong et al., "Measurements of the scattering coefficients of intralipid solutions by a femtosecond optical Kerr gate," *Opt. Eng.* **50**(4), 043607 (2011).
18. J. M. Khosrofian and B. A. Garetz, "Measurement of a Gaussian laser beam diameter through the direct inversion of knife-edge data," *Appl. Opt.* **22**(21), 3406–3410 (1983).
19. S. Moon, D. Kim, and E. Sim, "Monte Carlo study of coherent diffuse photon transport in a homogeneous turbid medium: a degree-of-coherence based approach," *Appl. Opt.* **47**(3), 336–345 (2008).
20. E. Berrocal et al., "Laser light scattering in turbid media. Part I: experimental and simulated results for the spatial intensity distribution," *Opt. Express* **15**(17), 10649–10665 (2007).

Shichao Xu received his MS degree in signal and information processing from Xi'an Shiyou University in 2012. He is currently pursuing his PhD degree with a focus on ultrafast time-gated ballistic-photon imaging in turbid media.

Biographies of the other authors are not available.